



## 저작자표시-비영리-변경금지 2.0 대한민국

이용자는 아래의 조건을 따르는 경우에 한하여 자유롭게

- 이 저작물을 복제, 배포, 전송, 전시, 공연 및 방송할 수 있습니다.

다음과 같은 조건을 따라야 합니다:



저작자표시. 귀하는 원저작자를 표시하여야 합니다.



비영리. 귀하는 이 저작물을 영리 목적으로 이용할 수 없습니다.



변경금지. 귀하는 이 저작물을 개작, 변형 또는 가공할 수 없습니다.

- 귀하는, 이 저작물의 재이용이나 배포의 경우, 이 저작물에 적용된 이용허락조건을 명확하게 나타내어야 합니다.
- 저작권자로부터 별도의 허가를 받으면 이러한 조건들은 적용되지 않습니다.

저작권법에 따른 이용자의 권리는 위의 내용에 의하여 영향을 받지 않습니다.

이것은 [이용허락규약\(Legal Code\)](#)을 이해하기 쉽게 요약한 것입니다.

[Disclaimer](#)

Thesis for the Degree of Master of Science

Prediction of Heavy Rainfall  
with the use of the High Resolution QPM  
over the Korean Peninsula

by

Ji-Hye Kim

Department of Environmental Atmospheric Sciences

The Graduate school

Pukyong National University

August 2012

Prediction of Heavy Rainfall  
with the use of the High Resolution QPM  
over the Korean Peninsula  
(고해상도 QPM 모델을 활용한 한반도  
집중호우 예측에 관한 연구)

Advisor: Prof. Jai-Ho Oh

by  
Ji-Hye Kim

A thesis submitted in partial fulfillment of the requirements  
for the degree of

Master of Science

in Department of Environmental Atmospheric Sciences

The Graduate School

Pukyong National University


August 2012




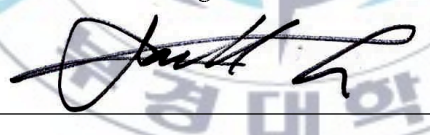
Prediction of Heavy Rainfall with the use of  
the High Resolution QPM over the Korean Peninsula

A dissertation  
by  
Ji-Hye Kim

Approved by:

  
\_\_\_\_\_  
(Chairman) Hyeong-Bin Cheong

  
\_\_\_\_\_  
(Member) Dong-In Lee

  
\_\_\_\_\_  
(Member) Jai-Ho Oh

August 24, 2012

# Contents

<b>List of Figures</b> .....	ii
<b>List of Tables</b> .....	vi
<b>Abstract</b> .....	V
<b>1. Introduction</b> .....	1
<b>2. Heavy rainfall cases and Model Description</b> .....	5
2.1. Cases of heavy rainfall events .....	5
2.2. Model description .....	7
<b>3. Experimental design and Forecast verification</b> .....	11
3.1. Experimental design .....	11
3.2. Forecast verification .....	19
<b>4. Results</b> .....	23
4.1. Total accumulated rainfall .....	23
4.2. 3-hour accumulated rainfall .....	34
<b>5. Summary and Conclusions</b> .....	40
<b>References</b> .....	44

# List of Figures

Fig. 1 Model simulation domains. : (a) WRF 8 km, the inner box indicates the subsequent nesting domain onto the WRF 2.6 km. (b) QPM 1 km. ....	15
Fig. 2 Experiment design. The experiments in (a) and (b) are QPM rainfalls directly disaggregated from GME simulation of 40 km and 20 km resolution, respectively. (c) and (d) are QPM rainfalls from 8 km WRF simulation (the outer domain) nested by GME simulation of 40 km and 20 km resolution (e) and (f) 2.6 km WRF simulation (the inner domain) forced by 8 km WRF simulation. ....	16
Fig. 3 Ratio of simulated rainfall amounts in accord with observation station to all observed rainfall for each event (a) and for all events averaged (b). ....	25
Fig. 4 Ratio of simulated rainfall amounts in accord with observation station to observed rainfall for the 200 mm threshold (a), for the 100 mm threshold (b) and for the 50 mm threshold (c) 30	
Fig. 5 The threat scores (a) and Bias scores (b) with respect to threshold values of total accumulated rainfall. ....	32
Fig. 6 The equitable threat scores (a) with respect to threshold values of total accumulated rainfall. ....	33

Fig. 7 Ratio of 3-hour area averaged rainfall to observation with times (a) and ratio of averaged rainfall to observation (b). .....	35
Fig. 8 Time series of a ratio of 3-hour peak rainfall to observation with times (a) and ratio of peak rainfall averaged time to observation (b). .....	37
Fig. 9 The equitable threat scores with respect to threshold values. ; 3 mm/3 hr (a), 5 mm/3 hr (b), 10 mm/3 hr (c) and 20 mm/3 hr (d). .....	39



## List of Tables

Table 1 Heavy rainfall events during the summer season (JJA) of 2011. ....	6
Table 2 Model (WRF) configuration of experiments. ....	14
Table 3 The name and process of each experiment. ....	17
Table 4 Integration time (unit : hour) taken to compute for a day (time step : 3-hour) for each process of experiments. Note that the number of cores for GME, WRF and QPM is 64, 64 and 16 respectively. ....	18





고해상도 QPM 모델을 활용한  
한반도 집중호우 예측에 관한 연구

김 지 혜

부 경 대 학 교 대 학 원 환 경 대 기 과 학 과

요 약

해상도가 증가함에 따라 강수예보가 향상되며, 특히 집중호우를 더 잘 모의함을 많은 연구에서 밝힌 바 있다. 그러나 컴퓨터 자원의 한계로 인해 수평해상도 1 km 이하의 NWP 모델을 활용한 연구가 거의 없다. 이에 본 연구에서는 역학적 과정은 포함되지 않았으나 강수에 중요한 요소 중 하나인 지형효과를 고려하여 적분시간을 단축시킬 수 있는 강수 진단 모형 (QPM)을 사용하였다. 강수진단 모형 (QPM)은 전지구모델 또는 지역모델의 강수예보를 배경장으로 사용하므로 강수 진단 모형 (QPM)의 배경장에 따라 어떤 결과가 도출되는지, 강수 진단 모형 (QPM) 배경장의 민감도 실험을 수행하는 것이 중요하다. 이에 본 연구에서는 고해상도 강수 진단 모형 (QPM)의 배경장으로써 모델의 해상도와 네스팅 기법이 강수 진단 모형 (QPM) 수행에 어떤 영향을 미치는지 알아보하고자 2011년 여름철 8개의 집중호우 사례에 대한 강수 진단 모형 (QPM) 결과를 분석하였다.

실험은 총 6가지로 구성된다. 40 km 전지구 모델 (GME)의 결과와 20 km 전지구 모델 (GME)의 결과 값에서 다운스케일링한 QPM의 결과와 40 km와 20 km 전지구모델 (GME)에서 한번 다운스케일링한 8km 지역 모델 (WRF)과 두 번 다운스케일링한 2.6 km 지역모델 (WRF)을 입력장으로 사용하는 QPM의 결과를 사용한다.

총 누적 강수량에 대한 강수분포와 peak rainfall을 분석하였으며, 정확도를 평가하기 위해 TS, ETS와 Bias score를 검증하였다. 총 누적 강수량에 대한 강수량 분포 분석에서는 지역모델을 한번 다운스케일링 한 QPM의 결과가 관측과 가장 유사한 모의를 보였으나, 200 mm가 넘는 강수량 분석에서는 지역모델을 두 번 다운스케일링 한 QPM의 결과가 관측과 가장 가까운 결과를 보였다. 하지만 임계값이 100 mm, 50 mm로 작아질수록 지역모델을 한 번 다운스케일링한 QPM의 결과 값이 관측과 가장 가까운 강수량을 보였다. 지역모델을 두 번 다운스케일링한 QPM의 결과가 peak rainfall을 가장 잘 모의하였으나 그 외 (상위 1 % 외) 강수량은 잘 모의하지 못했다. 이는 지역모델 내 역학과정이 반복 계산되면서 강수가 세분화되고 강화되었기 때문으로 사료된다. 전지구모델에서 다운스케일링 한 QPM의 TS, ETS는 임계값이 커질수록 값이 크게 감소하고 과소모의도 강하게 나타나 전지구모델에서

다운스케일링 한 QPM은 높은 임계값에서 좋지 못한 성능을 보였으나 지역모델에서 다운스케일링 한 QPM의 TS, ETS는 임계값이 커짐에도 값이 크게 감소되지 않고 높은 값을 유지하고 있어 높은 임계값에서 지역모델에서 다운스케일링 한 QPM이 탁월한 성능을 보임을 확인하였다. 지역모델 내 네스팅 수에 따른 ETS 결과의 차이는 크지 않았으나 지역모델을 한번 다운스케일링 한 QPM의 결과가 가장 우수하였다.

시간에 따른 QPM의 분석 결과, 전지구모델에서 지역모델을 한 번 다운스케일링한 QPM의 결과가 대부분 예보시간동안 관측과 가장 비슷한 값과 패턴을 생성하였으며, 특히 40 km 전지구모델에서 지역모델을 한 번 다운스케일링한 QPM이 가장 우수한 결과를 생성하였다. 시간에 따른 상위 1 % 내 강수량 분석에서는 예보시간에 따라 결과 값의 차이가 크게 나타났으며, 전반적으로 20 km 전지구모델에서 지역모델을 한 번 다운스케일링한 QPM의 결과와 20 km 전지구모델에서 지역모델을 두 번 다운스케일링한 QPM 결과가 시간별 peak rainfall의 양을 잘 모의하였다.

전지구모델의 결과 값이 QPM의 초기값으로 사용하는 경우 전지구모델의 해상도가 증가함에 따라 QPM의 결과 값도 크게 향상되었으나, 전지구모델에서 다운스케일링 한 지역모델의 결과 값을 초기값으로 사용하는 경우 전지구모델의 해상도 증가와 도출된 결과 사이의 상관성이 거의 없었다. 그러나 지역모델 자체 내 해상도 증가는 QPM의 peak rainfall 재생산에 탁월한 입력장 역할을 수행하였다. 하지만 전반적인 강수분포는 잘 모의하지 못하였다.

분석 결과, 40 km 전지구모델에서 지역모델을 두 번 다운스케일링 한 QPM과 20 km 전지구모델에서 지역모델을 한 번 다운스케일링 한 QPM의 예보정확도가 가장 높은 것으로 확인되었으나 시간 적분을 이용한 효율성을 고려할 시, 20 km 전지구모델에서 지역모델을 한 번 다운스케일링 한 QPM 예보가 가장 적절한 기법으로 사료된다.

# 1. Introduction

The Korean Peninsula often experiences heavy rainfall during summer. These heavy rainfall events are one of the main natural disasters over the Korean Peninsula. According to 10-year statistics(2000–2009), the damage to property caused by heavy rainfall events was 61% of the total property damage by nature disasters. Loss of life and property damage has increased from year to year (Park and Lee, 2011) Therefore, it is important to forecast the timing and distribution of these heavy rainfall events accurately.

There have been many studies to improve the rainfall forecast ability. Most studies have shown that increasing horizontal resolution could improve the simulation and reproduce results more similar to the rainfall observation. Mass et al. (2002) suggests that increasing the resolution from 12 to 4 km caused further finer-scale improvements, compared to the improvements in mesoscale structures as the grid spacing decreases from 36 to 12 km. Lee et al. (2004) found improved heavy rainfall patterns and amounts associated with the June 1998 East Asian flood through the better-simulated downward solar radiation, convective rainfall after the grid size was reduced from 60 to 20 km. Later, Xue et al. (2007) showed that RCMs could produce better the rainfall distribution over North America when the grid size

is reduced from 80 to 32 km. Recently Shin and Hong (2009) investigated that the high-resolution WRF model is capable of reproducing the observed record-breaking rainfall fairly well, both in intensity and distribution with concentrated rainfall on Jeju Island. Lee et al. (2011) illustrated that the accuracy of the heavy rainfall forecasts improved considerably with increasing horizontal resolution in the case of large synoptic forcing. However to our knowledge, a few studies have utilized NWP model using a grid size of less than 1 km because of computer resources.

Diagnostic rainfall model is utilized for reproducing fine-mesh rainfall at a resolution of 1 km. It has an advantage of avoiding a huge amount of integration time because dynamical processes in the atmosphere are not included in reproducing fine-mesh rainfall. It utilized the meteorological fields derived from either global or local model as background, then disaggregate rainfall onto a finer scale by considering orography effect.

Previous studies have already tested the performance of the diagnostic rainfall model (QPM). Kim (2004; in Korean) showed detailed rainfall information with 3 km horizontal resolution and a better capability of diagnostic rainfall compared to mesoscale model. Again, Kim et al. (2008) suggested that the forecast of heavy rainfall as well as its spatial distribution has shown good agreement with the observed ones and better results in predicting the peak rainfall

amounts than those given by the Regional Data Assimilation Prediction System (RDAPS). Recently Jung (2010; in Korean) found that QPM captures the pattern of annual total precipitation, the seasonal changes in precipitation and the rain days in summer as well as the heavy rainfall frequency in summer.

Previous studies identified excellent performance of diagnostic rainfall model (QPM). They utilized the meteorological fields derived from either global or model as background. Therefore importance of background of the QPM should be taken into account in terms of accuracy and efficiency. Kim and Oh (2010) has already performed a series of experiments designed with both NWP models and a diagnostic rainfall model to examine importance of input data in the diagnostic rainfall model in reproducing the heavy rainfall event. It is found that QPM forecast from 20 km global run displays similar results to the one from 7.8 km local model run derived by 40 km global model run. When computational time is considered, it may be concluded that the modeling system which couples 40 km global-7.8 km local models and the diagnostic rainfall model turned out to be the best nesting approach. However a single case have demonstrated to examine the performance of QPM forecast in them. Therefore in this study, prediction of QPM for the recent heavy rainfall events have been analyzed based on experimental design of kim and Oh (2010).

The objective of this study is to investigate the potential role of

the resolution of background models and nesting process in high-resolution diagnostic rainfall model for the recent heavy rainfall events and to evaluate the forecast accuracy of the diagnostic rainfall model run over the Korean peninsula together with time efficiency.



## 2. Heavy rainfall cases and Model Description

### 2.1. Cases of heavy rainfall events

Eight heavy rainfall events which occurred over the Korean peninsula during the summer season (JJA) of 2011 were used. These events represent typical heavy rainfall events that occur over the Korean peninsula. These are relative to synoptic scale disturbances on the Changma front, mesoscale convective systems between the continental lows over china and North Pacific subtropical highs. Detailed information about each event is found in climatological statistics analysis data by KMA (2011).





Table 1 Heavy rainfall events during the summer season (JJA) of 2011.

No.	Initial time (UTC)	Count of AWS data
1	2011062300	600
2	2011062412	615
3	2011062800	593
4	2011070812	619
5	2011072600	574
6	2011073012	612
7	2011080612	601
8	2011080812	609





## 2.2. Model description

In this study, a global model and regional model was used together with a diagnostic rainfall model. Description of each model is briefly summed up as follows.

### (1) GME (Global Model)

GME is operational global numerical weather prediction model developed by German Weather Service (Deutscher Wetterdienst). The grid of GME is generated by inscribing an icosahedron with 20 triangles of equal size into the sphere. The spacing of the icosahedral – hexagonal grid of the GME is determined by the parameter  $ni$  which is the number of intervals on a main triangle side. that is, each edge of the 20 spherical triangles is subdivided into  $ni$  parts until the grid spacing reaches the target resolution. the icosahedral – hexagonal grid of the GME has advantage of avoiding the so-called pole problem that exists in conventional latitude – longitude grids and the large amount of global communication required by spectral transform techniques as the resolution increases. It also provide a data structure extremely well suited to high efficiency on distributed memory parallel computer (Majewski et al., 2002).

## (2) WRF (Regional Model)

The Advanced Research WRF (ARW; Skamarock et al., 2005) is a community model suitable for both research and forecasting. WRF is a fully compressible, Euler nonhydrostatic model using a terrain-following hydrostatic pressure vertical coordinate. The horizontal grid is an Arakawa C grid. For integrating the equations, a third-order Runge-Kutta scheme is used.

## (3) QPM (Quantitative Precipitation Model)

Quantitative Precipitation Forecasting (QPM) is diagnostic rainfall model based on Collier-type suggested by Misumi et al. (2001), Bell (1978) and Collier (1975). It utilizes the meteorological fields derived from either global or local model as background and then disaggregates rainfall onto a finer scale by considering orography effect.

The mass of raindrops per unit mass of dry air, named  $Q_r$ , is shown by Eq. (1).

$$\frac{\partial Q_r}{\partial t} = u \frac{\partial Q_r}{\partial x} - v \frac{\partial Q_r}{\partial x} - w \frac{\partial Q_r}{\partial x} + \frac{1}{\rho} \frac{\partial}{\partial z} (\rho V_r Q_r) + P_1 - E_1 \quad (1)$$

Where,  $x$ ,  $y$  and  $z$  are space coordinates,  $t$  is time,  $u$ ,  $v$  and  $w$  are the components of wind in  $x$ ,  $y$ ,  $z$  directs.  $\rho$  is the density of the

air,  $V_r$  is the terminal fall speed of the raindrop,  $P_1$  and  $E_1$  are the condensation and evaporation rate.

$$\begin{aligned} \frac{\partial(\overline{Q_r + Q'_r})}{\partial t} = & u \frac{\partial(\overline{Q_r + Q'_r})}{\partial x} - v \frac{\partial(\overline{Q_r + Q'_r})}{\partial x} - w \frac{\partial(\overline{Q_r + Q'_r})}{\partial x} \\ & + \frac{1}{\rho} \frac{\partial}{\partial z} (\rho V_r (\overline{Q_r + Q'_r})) + (\overline{P_1 + P'_1}) - (\overline{E_1 + E'_1}) \end{aligned}$$

(2)

Air density and wind components in Eq. (1) are assumed to be the same as those in the global or regional fields. Physical terms of  $Q_r$ ,  $P_1$  and  $E_1$  are split into two parts, the large-scale mean fields (indicated by overbars in Eq. (2)) and small-scale perturbations (indicated by primes in Eq. (2)), using a technique similar to that developed by Stein and Nordlund (1991). The terminal fall speed of raindrops  $V_r$ , is not separated because the raindrops produced by the mesoscale forcing and by the small-scale perturbation are assumed to fall together with the same speed. The Perturbation terms represent small-scale terrain effect. When assuming that atmosphere is in steady state,  $Q'_r$  is the differential mixing ratio occurred between additional condensation ( $P'_1$ ) and evaporation ( $E'_1$ ) due to the forcing from the terrain. For calculating rain drop movement easily, terrain-following coordinate is used.

Finally the rainfall intensity,  $I$ , can be obtained as

$$I = V_r(\overline{Q_r} + Q_r') \quad (3)$$

The detailed formulation and process of the QPM can be found in Kim et al. (2008), Jung (2010) and Kim and Oh (2010).



### 3. Experimental design and Forecast verification

#### 3.1. Experimental design

Experimental design are the same as those by Kim and Oh (2010), except for regional model and the grid size used for the domain of regional model and diagnostic rainfall model.

The global model (GME) has been run at a resolution of 40 km/40 layers (ni=192) and 20 km/40 layers (ni=384) using operational ECMWF data as initial data (T511L91).

Regional Model (WRF) has been run using two-nested domains. 8 km grid domain is used as the outer domain. 2.6 km grid domain was nested inside a 8 km grid domain by a one-way interaction. Simulation of GME was used as the initial and boundary conditions. Boundary conditions were updated every 3 hour. The whole grid systems had 28 vertical layers and model top was located at 50 hPa. The Rapid Radiative Transfer Model (RRTM) scheme (Mlawer et al., 1997) for the parameterization of longwave radiation, combined with the cloud radiation shortwave scheme (dudhia, 1989) was used for radiation parameterization. The Yonsei University (YSU) planetary boundary layer (hong et al., 2006), based on Non-local-K scheme with

explicit entrainment layer and parabolic K profile in unstable mixed layer, was used for PBL processes. The WSM6 microphysics scheme (Hong and Lim, 2006) with which ice, snow and graupel processes suitable for high-resolution simulations. The newest version of the Kain-Kritsch (KF2) convective parameterization scheme (CPS) was used for subgrid-scale convection including the effects of shallow convection (Kain, 2004). Inner domain (2.6 km grid domain) was performed with same physics schemes except cumulus parameterization (CPS). CPS is needed for 3-10 km horizontal resolutions, because they could not resolve even the largest supercell storms of about 6-10 km. In this study, coarse domain (8 km grid domain) only employed CPS. Table 2 presents the WRF configuration used in this study.

A diagnostic rainfall model (QPM) has been run at 1 km resolution for utilizing high-resolution information of heavy rainfall. Because rainfall in the QPM mostly depends on the background physical field from coarser model and is added to the background by considering orography effect, it is always greater than or equal to the rainfall from the background. Therefore it is important to compare the performances of QPM produced by multiple nesting in the NWP model with time efficiency and forecast accuracy.

The model domain of WRF and QPM used in the present study is shown in Fig. 3. The first 6 hour integrations are treated as the model spinup, therefore they are not used for the model analysis.

The experimental design in this study is comprised of six experiments and is shown in Fig. 3 and the name and process of each experiment are given in Table 2. The experiments in Fig. 4a and 4b are QPM rainfalls directly disaggregated from GME simulation of 40 km and 20km resolution, respectively. Figs. 4c and 4d are QPM rainfalls from 8 km WRF simulation (the outer domain) nested by GME simulation of 40 km and 20 km resolution while Figs. 4e and 4f are those from 2.6 km WRF simulation (the inner domain) forced by 8 km WRF simulation. These experiments are referred to as G4Q1, G2Q1, G4W8Q1, G2W8Q1, G4W2Q1 and G2W2Q1, respectively.

All global and region model have been run using 64 CPU located in KISTI (Korea Institute of Science and Technology Information)/supercomputing center. There is huge difference of integration time used by using which nesting process when producing high-resolution information (Table 4). For example, Difference of integration time of G4Q1 and G2W2Q1 is over 20 times. If there are no or only a little differences in the accuracy between two groups, the coupled model system which needs less computational time can save much time and resources (Kim and Oh, 2010).



Table 2 Model (WRF) configuration of experiments.

	Domain 1	Domain 2
Horizontal dimensions	363 × 363 (8km)	322 × 322 (2.6km)
Vertical layers/Model Top	28 sigma layers/50hPa	
Cumulus parameterization	Kain-Fritsch 2	–
Radiation parameterization(SW/LW)	Dudhia/RRTM	Dudhia/RRTM
Microphysical parameterization	WSM6	WSM6
PBL/turbulence parameterization	YSU	YSU





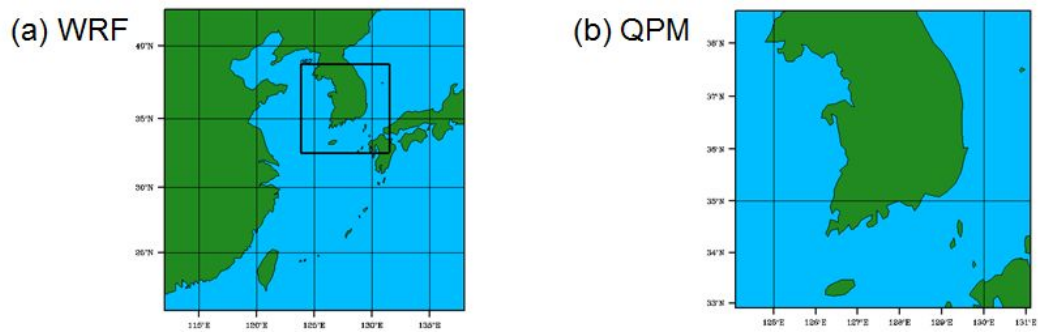


Fig. 1 Model simulation domains. : (a) WRF 8 km, the inner box indicates the subsequent nesting domain onto the WRF 2.6 km. (b) QPM 1 km.



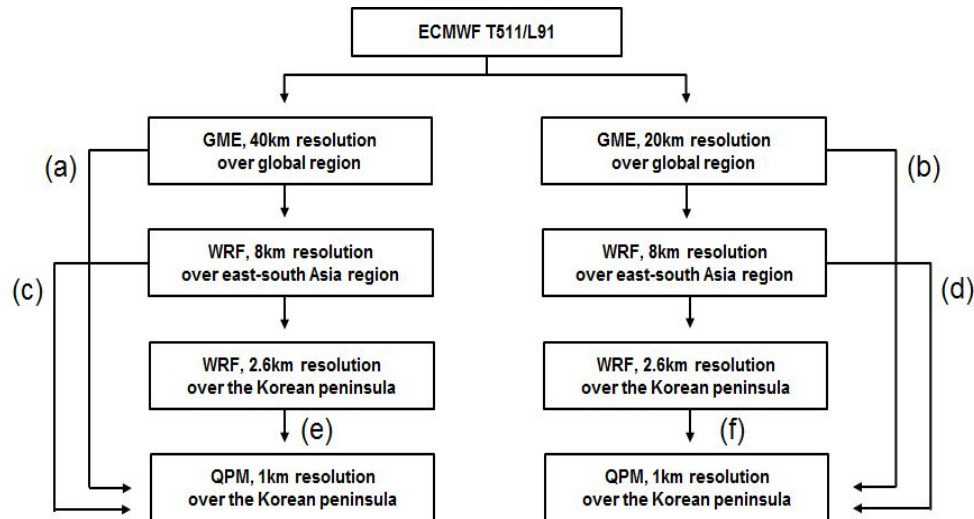


Fig. 2 Experiment design. The experiments in (a) and (b) are QPM rainfalls directly disaggregated from GME simulation of 40 km and 20 km resolution, respectively. (c) and (d) are QPM rainfalls from 8 km WRF simulation (the outer domain) nested by GME simulation of 40 km and 20 km resolution (e) and (f) 2.6 km WRF simulation (the inner domain) forced by 8 km WRF simulation.



Table 3 The name and process of each experiment.

Experiment name	Process of Model simulation			
(a) G4Q1	GME 40km			QPM 1km
(b) G2Q1	GME 20km			QPM 1km
(c) G4W8Q1	GME 40km	WRF 8km		QPM 1km
(d) G2W8Q1	GME 20km	WRF 8km		QPM 1km
(e) G4W2Q1	GME 40km	WRF 8km	WRF 2.6km	QPM 1km
(f) G2W2Q1	GME 20km	WRF 8km	WRF 2.6km	QPM 1km



Table 4 Integration time (unit : hour) taken to compute for a day (time step : 3-hour) for each process of experiments. Note that the number of cores for GME, WRF and QPM is 64, 64 and 16 respectively.

	GME 40 km (h/day)	GME 20 km (h/day)	WRF 8 km (h/day)	WRF 2.6 km (h/day)	QPM 1 km (h/day)	TOTAL (h/day)
(a) G4Q1	0.93				0.13	1.06
(b) G2Q1		4.67			0.13	4.8
(c) G4W8Q1	0.93		3.73		0.13	4.79
(d) G2W8Q1		4.67	3.73		0.13	8.53
(e) G4W2Q1	0.93			15.2	0.13	16.26
(f) G2W2Q1		4.67		15.2	0.13	20



## 3.2. Forecast verification

In order to verify model forecast, observation data, the automatic weather station (AWS) data which has an average station spacing of 15 km, was used. The AWS station with missing values are not used. The number of AWS data selected was given in Table 1 case by case.

When the comparison between AWS data and model forecast is performed, one has to be aware of the different quantities: AWS data are point measurements, whereas model forecast represents an areal mean. Therefore, model forecast is interpolated at all AWS observation points.

Counts for forecast/event pairs for the dichotomous categorical verification situation was calculated based on  $2 \times 2$  contingency table. Following four categories are defined relative to some specific rain threshold values : The number of points where model predicted rain and rain occurred (A), the number of points where model predicted rain but rain did not occur (B), the number of points where rain occurred but model failed to predict rain, the number of points where model predicted rain and rain did not occurred.

Perfectly accurate forecasts in the  $2 \times 2$  categorical forecasting situation will clearly exhibit  $b=c=0$ , with all "yes" forecasts for the event followed by the event and all "no" forecasts for the event

followed by nonoccurrence. For real, imperfect forecasts exist mostly. Therefore measures are needed to discern degrees of accuracy. Several scalar measures are in common use, with each reflecting somewhat different aspects of the underlying joint distribution. In this study, threat scores (TS), equitable threat scores (ETS) are used.

The threat score (TS) is used when the event to be forecast occurs substantially less frequently than the nonoccurrence. It is computed as

$$TS = \frac{A}{A+B+C}$$

(4)

The threat score is the number of correct "yes" forecasts divided by the total number of occasions on which that event was forecast and/or observed. The worst possible threat score is zero, and the best possible threat score is one.

The equitable threat scores (ETS; Schaefer, 1990) is the fraction of observed and/or forecast events that were correctly predicted, adjusted for hits associated with random chance. The ETS is often used in the verification of rainfall in NWP models because its "equitability" allows scores to be compared more fairly across different regimes. It is sensitive to hits. Perfect forecasts receive one, forecasts

equivalent to the reference forecasts receive zero scores, and forecasts worse than the reference forecasts receive negative scores. It is computed as

$$ETS = \frac{A - R_{ram}}{A + B + C - R_{ram}} \quad (5)$$

The reference accuracy measure ( $R_{ram}$ ) represents that part of the forecast obtained by chance and given by

$$\text{where } R_{ram} = \frac{(A+B)(A+C)}{A+B+C+D} \quad (6)$$

The bias, or comparison of the average forecast with the average observation, of categorical forecasts, is usually represented as a ratio. Bias is not an accuracy measure because it isn't correspondence between the forecasts and observations of the event on particular occasions. But it can distinguish overforecasting and underforecast. Bias greater than one indicates that the event was forecast more often than observed, which is called overforecasting. Conversely, bias less than one indicates the event was forecast less often than observed, or was underforecast. The bias ratio is given by

$$B = \frac{A+B}{A+C}$$

(7)





## 4. Results

### 4.1. Total accumulated rainfall

#### (a) Area-averaged rainfall

Figure 3 shows the ratio of simulated rainfall amounts in accord with observation station to all observed rainfall for each event (a) and for all events averaged (b). Noticeable improvement from change in horizontal resolution of global model as direct input of QPM were found in all events. The QPM results derived by a higher resolution (20 km) of global model and those derived by the single nesting regional model (Fig. 2c and 2d) are similar to observation. These results may be due to physically recalculation in regional model. Regional model recalculate atmosphere fields smaller than what is resolvable on a global scale. More detailed information as input of QPM is given by regional model. That's why QPM results derived by the regional model improve on those derived by the global model in some events. However, if more detailed information is miscalculated and misdistributed by interaction between differential vorticity advection, upper-level divergence and so on in regional model, QPM results derived by the regional model is degraded. In this case, QPM

results derived by the global model show better than other experiments.

Figure 3 (b) shows QPM result (G2W8Q1) derived by the single nesting regional model in a higher global model is reproduced more, showing no significant differences when comparing with that (G4W8Q1) in a lower global model. QPM result derived by double nesting regional model (Fig. 2e and 2f) produce less rainfall amounts than that by single nesting regional model (Fig. 3 (b)). One notices that QPM results using double nesting in regional model does not necessary yield more accurate rainfall amounts in terms of distribution.



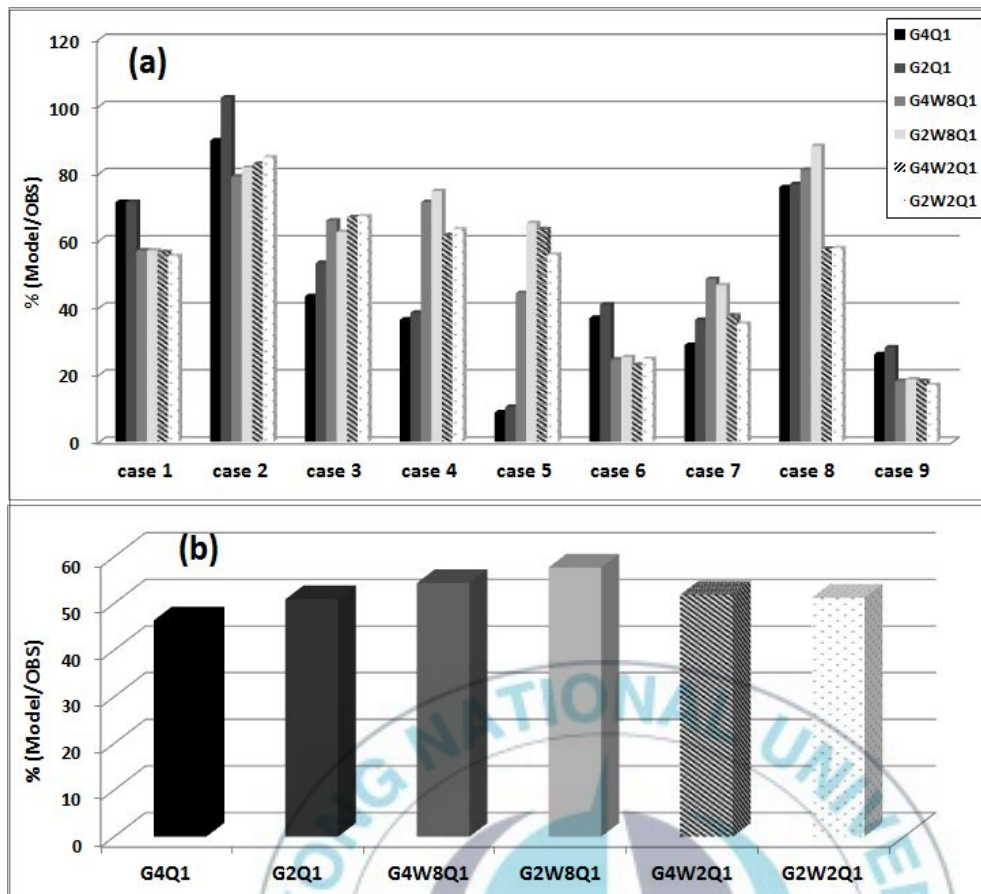


Fig. 3 Ratio of simulated rainfall amounts in accord with observation station to all observed rainfall for each event (a) and for all events averaged (b).

(b) Peak rainfall amounts

To analyze capability of QPM in terms of peak rainfall, rainfall amounts were calculated for given thresholds. Figure 4 shows ratio of simulated rainfall amounts in accord with observation station to observed rainfall for the 200 mm threshold (a), for the 100 mm threshold (b) and for the 50 mm threshold (c).

Regardless of given thresholds, as grid spacing of global model decrease, QPM results which originated from the forcing by global model and derived by single nesting regional model were improved, while QPM results (G4W2Q1) derived by double nesting regional model were not improved. These results support conclusion that resolution of global model in double nesting regional model have little impact on the rainfall recalculation in the QPM.

QPM result derived by double nesting regional model showed the highest percentage among the other experiments for the 200 mm threshold (Fig. 4(a)). That is, it mean G4W2Q1 and G2W2Q1 results which forced by double nesting in regional model offer sufficient peak rainfall information than other experiment. Background information of higher resolution has an advantage in resolving the peak rainfall for the high threshold. These results were same to those from analysis of peak rainfall in top 1 % (not shown). QPM results are like those obtained in Figure 3 for the lighter thresholds (50 and 100 mm). Ratio

of QPM result derived by single nesting regional model (G2W8Q1) to observation was the highest percentage for 100 mm threshold. However there was no much different between QPM results derived by single nesting region model and those derived by double nesting regional model. That is why ratio of QPM results which derived by double nesting regional model to observation decreased (decrease of G4W2Q1 and G2W2Q1 is -1.55, -1.34 respectively), while that of other QPM results increased. There was improved ratio at all experiments for 50 mm threshold compared to 100 m threshold. However overall pattern of all experiments is similar to that produced for 100 mm threshold. QPM result (G2W8Q1) derived by single nesting regional model is the closest value with observation for 50 and 100 mm threshold.

According to the results, QPM result (G4W2Q1) derived by double nesting regional model from coarser resolution of global model is appropriate of reproducing peak rainfall amounts (above 200 mm or in top 1 %). However QPM result (G2W8Q1) derived by single nesting regional model from higher resolution of global model reproduced the rest of rainfall amounts (except above 200 mm). It is because denser rainfall is calculated at QPM due to double nesting in regional model as QPM background.

When considering the results of the analysis and definition that heavy rainfall is mainly used a word to indicate rainfall above 80 mm

per day, QPM result (G2W8Q1) derived by single nesting regional model is also the most appropriate of reproducing peak rainfall amounts.





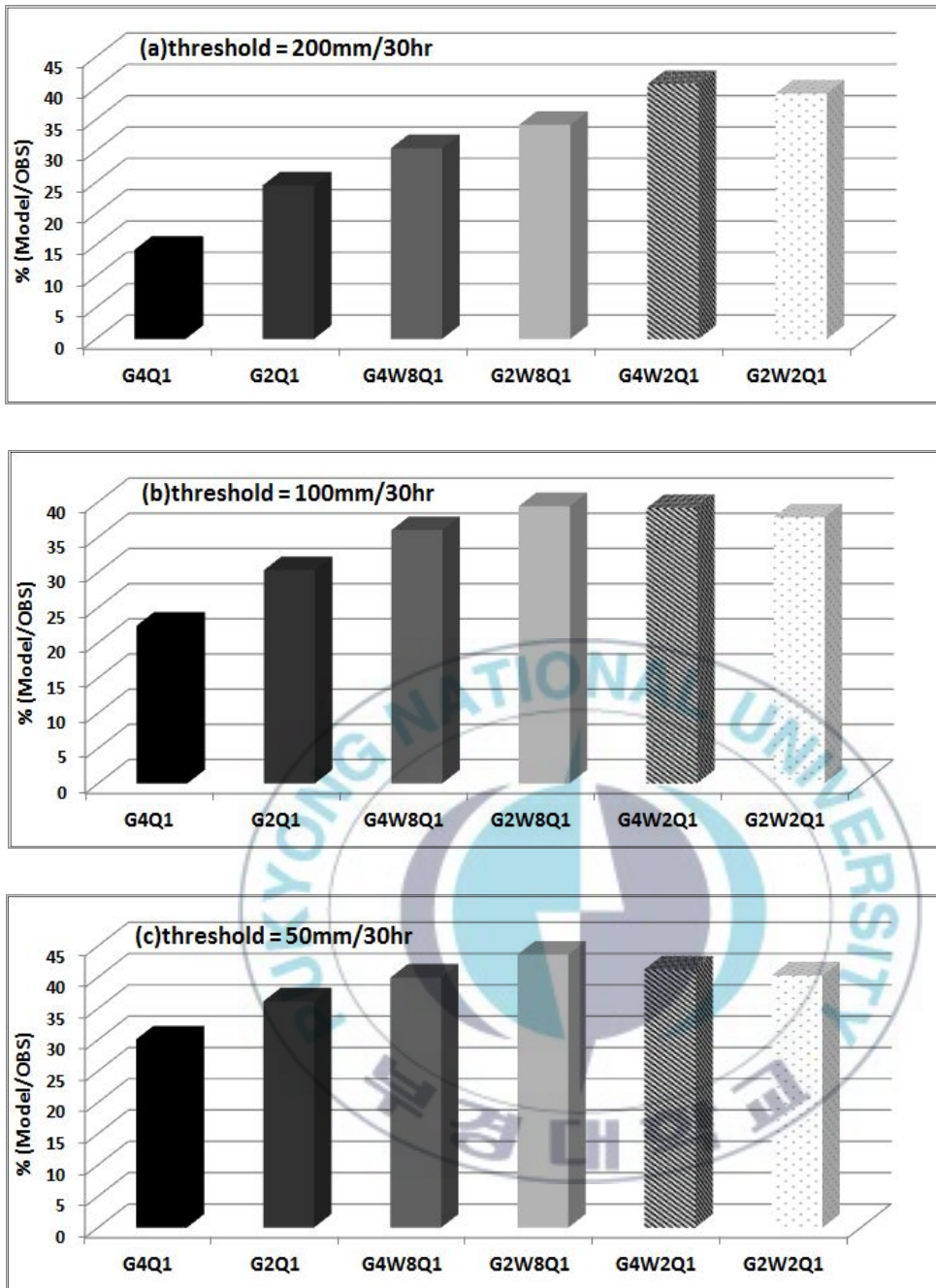


Fig. 4 Ratio of simulated rainfall amounts in accord with observation station to observed rainfall for the 200 mm threshold (a), for the 100 mm threshold (b) and for the 50 mm threshold (c).

## (b) Forecast Verification

In order to quantitatively access the performance of QPM, TS, ETS, BIAS were calculated at some specific thresholds of rainfall amounts for all eight cases and those are averaged. Figure 5 shows the TS (a) and Bias Score (b) for the thresholds at five intervals. No significant differences of TS among all experiments found for the lighter thresholds. As threshold increase, difference of TS among all experiments became bigger. QPM results derived by double nesting regional model showed the greatest accuracy for most thresholds (Fig. 5(a)). It is considered as QPM results derived by double nesting regional model reproduce peak rainfall well (Fig. 4 (a)). Figure 6 shows the ETS (a) for the thresholds at five intervals. The ETS adjusted for hits associated with random chance shows a fairly great difference compared to TS. QPM results (G2W8Q1) derived by single nesting region model from higher resolution have highest ETS for most thresholds (Fig. 5 (a)). These results are different to that of TS.

Because ETS exclude hits associated with random chance, QPM results (derived by double nesting regional model) that showed a higher score at TS may be considered as hits is high by random chance.

QPM results originated from global model simulated better than other those for lighter threshold (below 20 mm threshold). However



QPM results originated from global model show the lowest score among other those for higher threshold. As threshold increase, they have decreased considerably, especially that (G4Q1) from a lower resolution of global model. These results were consistent with bias scores. They show good performance for lighter threshold but have the lowest bias scores (underforecast) for the high thresholds. G2Q1 result of them is improved by increasing the resolution of global model. However, In spite of improvement, its performance is not good in comparison with other QPM results produced using regional model.

Because QPM utilized meteorological field from results of large scale and disaggregate rainfall onto a finer scale by considering orography effect, rainfall produced using QPM improved compared to that using only global model. However, due to coarser grid of global model, rainfall is incapable of expression at resolution of global model (in this case physical parameterization is needed) and it is also not calculated at QPM. Whereas in case of calculating physical processes at higher resolution through regional model, rainfall is recalculated utilizing them in QPM. Therefore this problem, reproducing heavy rainfall, may seem to be resolved when background of QPM use results of regional model. Therefore results of global model is not sufficient to reproducing fine-mesh rainfall.

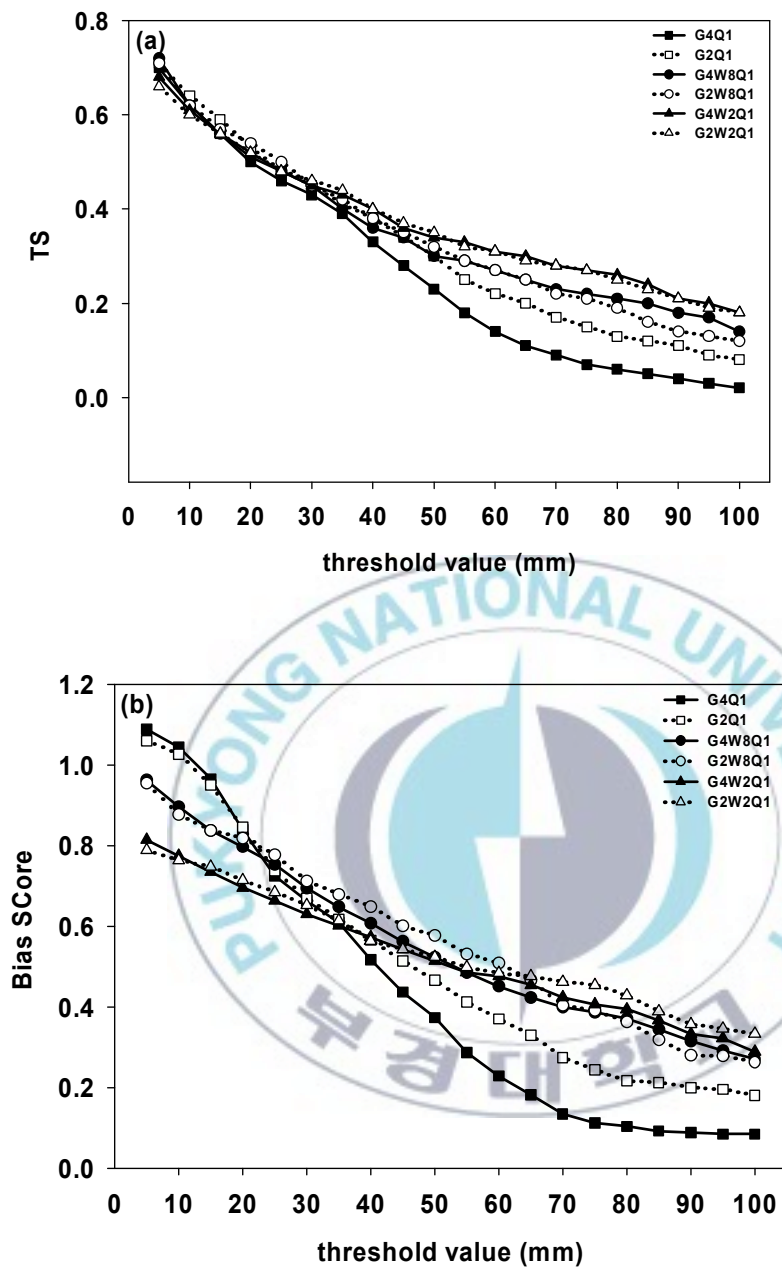


Fig. 5 The threat scores (a) and Bias scores (b) with respect to threshold values of total accumulated rainfall.

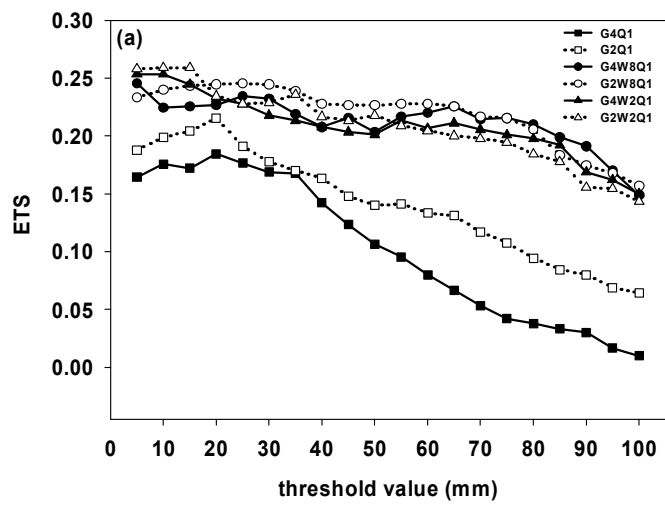
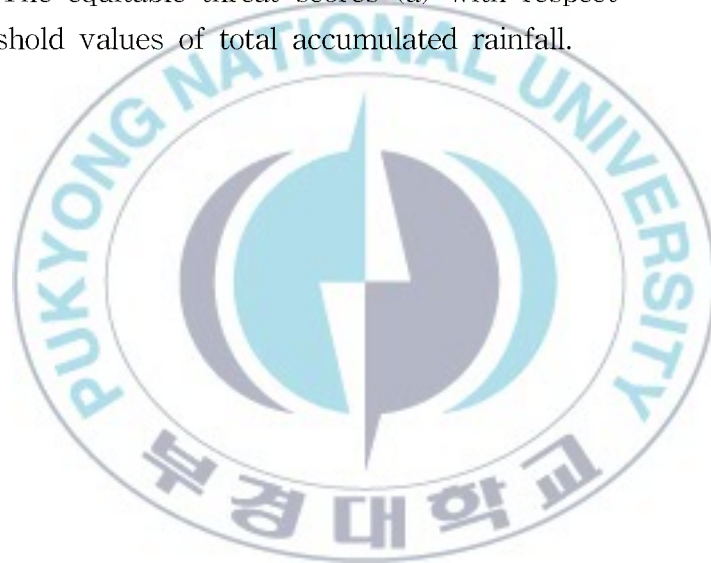


Fig. 6 The equitable threat scores (a) with respect to threshold values of total accumulated rainfall.



## 4.2. 3-hour accumulated rainfall

### (a) Temporal distribution.

Area averaged rainfall amounts of all QPM's with time are investigated. Figure 7 shows a time series of a ratio of 3-hr area averaged rainfall to observation. The ratio of 3-hr area averaged rainfall to total observed rainfall was calculated case by case, then the ratios were averaged for all events. Temporal variation of all simulated experiment results agrees well with that of observed rainfall amount. However all experiments can not reproduce rainfall amounts at 27 forecast time which appear to second peak rainfall. QPM results (G2W8Q1 and G4W8Q1) nested from single nesting regional model show better performance with time. Especially G4W8Q1 show a similar observed rainfall amounts, while QPM results (G2Q1 and G4Q1) show worse performance with time. Gap of difference of QPM results (G2W8Q1 and G4W8Q1) derived by single nesting region model and those (G2W2Q1 and G4W2Q1) derived by double nesting region model became smaller than that of total accumulated rainfall (Fig. 7 (b)). However G2W8Q1 and G4W8Q1 show still better performance with time than G2Q2Q1 and G4W2Q1 in terms of distribution of rainfall.

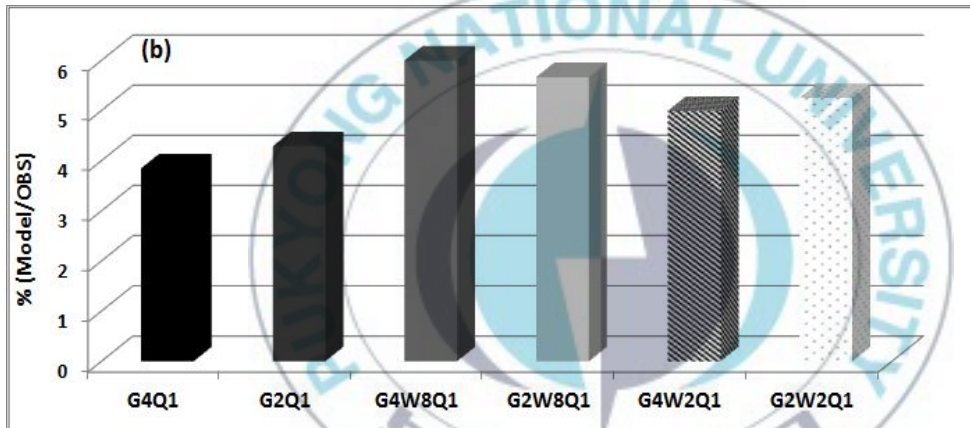
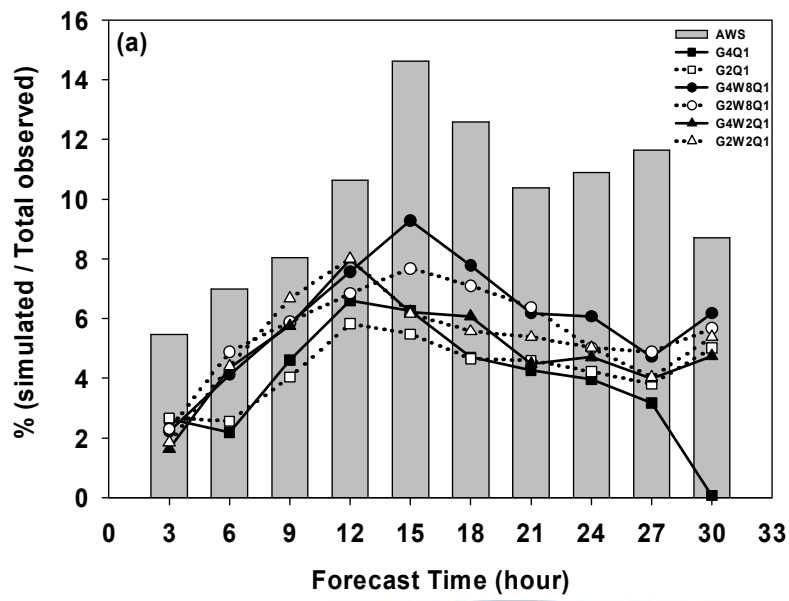


Fig. 7 Ratio of 3-hour area averaged rainfall to observation with times (a) and ratio of averaged rainfall to observation (b).

(b) Temperately peak rainfall

Peak rainfall amounts of all QPM's with time is investigated. Peak rainfall amounts is defined as rainfall amounts in top of 1 %. Figure 8 shows a time series of a ratio of 3-hour peak rainfall to observation. The ration of 3-hour peak rainfall to observed rainfall was calculated case by case, then the ratios were averaged for all events. In case of peak rainfall, performance of all QPM depends on forecast time. QPM results (G2W2Q1 and G4W2Q1) derived by double nesting regional model show better during 0-15 time periods, while QPM results (G2W8Q1 and G4W8Q1) derived by single nesting regional model are similar to observation during 15-30 time periods. When averaged all forecast time, G2W8Q1 and G2W2Q1 are the closest vale to observation than other experiments. These results are different from those analyzed with total accumulated rainfall which QPM results derived by double nesting regional model show the best in analysis of total accumulated rainfall.

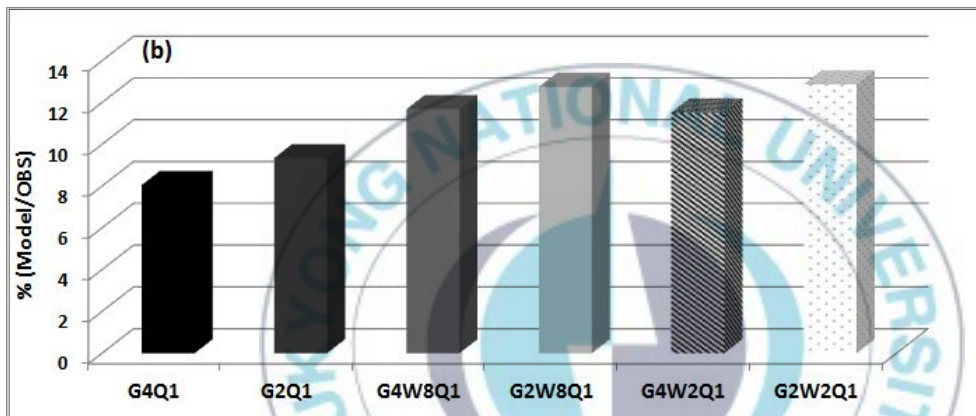
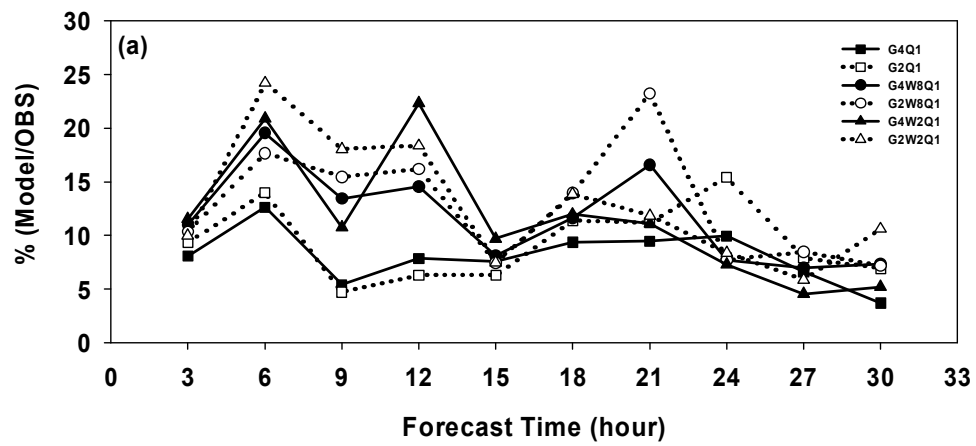


Fig. 8 Time series of a ratio of 3-hour peak rainfall to observation with times (a) and ratio of peak rainfall averaged time to observation (b).



(c) Temperately forecast verification

ETS was calculated at four threshold values (3 mm/3 hr, 5 mm/3 hr, 10 mm/3 hr, 20 mm/3 hr) of rainfall amounts for all eight cases, then those are averaged. QPM results (G4Q1 and G4W8Q1) nested from a lower global model show better than other results for low thresholds, while those (G2Q1 and G2Q8Q1) nested from a higher global model show better. However QPM results (G2W2Q1 and G4W2Q1) derived by double nesting regional model do not have correlation between resolution global model and thresholds. G2Q1 and G4Q1 have high score at 15 hour which comes to first peak rainfall. However, outside those hours, performance of those were the lowest. Those completely could not capture rainfall for 20 mm/3 hr threshold, These results are consistent with analysis of total accumulated rainfall. All of QPM results show better performance at first peak rainfall (15 hour) which is shown in Fig. 7. But those show weak performance at second peak rainfall (27 hour).



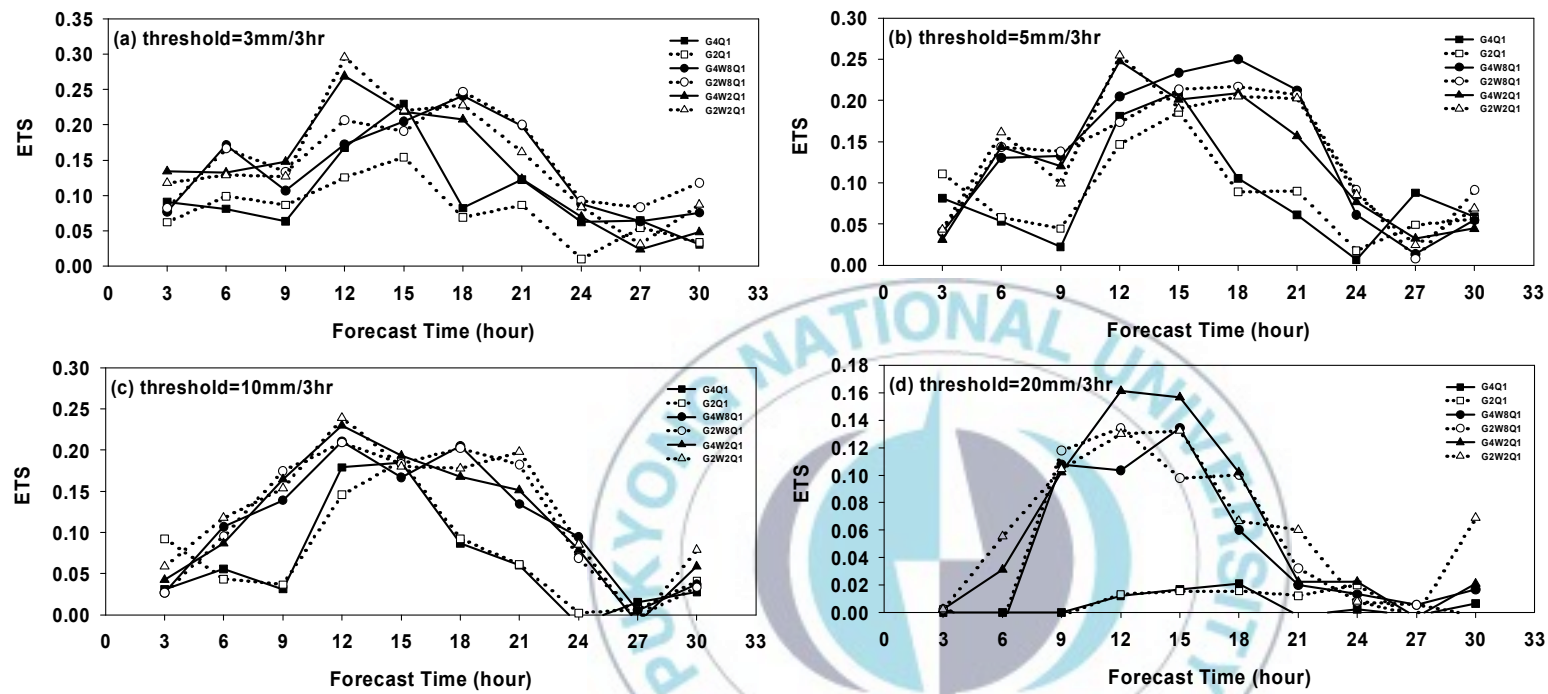


Fig 9 The equitable threat scores with respect to threshold values. ; 3 mm/3 hr (a), 5 mm/3 hr (b), 10 mm/3 hr (c) and 20 mm/3 hr (d).

## 5. Summary and Conclusions

The objective of this study is to examine capability of high resolution QPM and decide the most appropriate nesting process in terms of the rainfall intensity, distribution and considering efficiency. In this study, to complement results of Kim and Oh (2010), prediction of QPM for many of the recent heavy rainfall events have been analyzed as suggested by them. Recent heavy rainfall events was used eight heavy rainfall events which occurred over the Korean peninsula during the summer seaseon (JJA) of 2011. The experiment design consists of six experiments; QPM rainfalls directly disaggregated from global model simulations of 40 km and 20km resolution, respectively. QPM rainfalls from 8 km regional simulations (the outer domain) nested by global model simulations of 40 km and 20km resolution while those from 2.6 km regional model simulations (nested domain) forced by 8 km regional simulations.

The analysis of area-averaged rainfall have been carried out. Noticeable improvement from change in horizontal resolution of global model as direct input of QPM were found in all events. QPM result (G2W8Q1) derived by the single nesting regional model in a higher global model is reproduced the most. QPM result derived by double nesting regional model produce less rainfall amounts than that by single nesting regional model.

The evaluation of peak rainfall have been examined. QPM result derived by double nesting regional model showed highest percentage among the other experiments for the 200 mm threshold. That is, it mean G4W2Q1 and G2W2Q1 results offer sufficient peak rainfall information than other experiments, which forced by double nesting in regional model. Background information of higher resolution has an advantage over that of coarser resolution in resolving the peak rainfall for the high threshold. QPM results like those obtained in results of area averaged rainfall were computed for the lighter thresholds (50 and 100 mm).

For verification of simulated rainfall amount, TS , Bias score and ETS was calculated. No significant differences of TS among all experiments found for the lighter thresholds. As increase threshold, differences among all experiments grows. QPM results derived by double nesting regional model show the greatest accuracy. In results of ETS, QPM results (G2W8Q1) derived by single nesting region model from higher resolution have highest ETS for most thresholds.

It is important for which experiments to simulate peak rainfall and distribution of rainfall with time. Time series of all experiments also have been carried out. Gap of difference of QPM results (G2W8Q1 and G4W8Q1) derived by single nesting region model and those (G2W2Q1 and G4W2Q1 ) derived by double nesting region model became smaller than that of total accumulated rainfall (Fig. 7

(b)). However G2W8Q1 and G4W8Q1 show still better performance with time than G2Q2Q1 and G4W2Q1 in terms of distribution of rainfall. In analysis of rainfall in top of 1 %, G2W8Q1 and G2W2Q1 is the closest value to observation than other experiments. QPM results nested from global model completely can not capture rainfall for 20 mm/3 hr threshold. It is consistent with analysis of total accumulated rainfall.

When comparing the global effects and local effects in QPM, QPM results nested from regional model show better performance than those nested from only global model. High resolution regional model as input of QPM give more accurate peak rainfall but that show larger spread and variance. Therefore the increase of horizontal resolution up to 2.6 km in WRF runs induces a deterioration of distribution of rainfall.

When taking into consideration of correlation between resolution of global model and improvement of rainfall in QPM, As increase resolution of global model, performance of QPM results derived from global model as input is also improved. However that of QPM results derived from regional model as input have nothing to do with resolution of global model. It may be due to itself recalculation physically in regional model. Therefore these results are found much more in QPM results using double nesting in regional model.

When considering forecast accuracy and time efficiency, it may

be concluded that QPM forecast from 8 km regional model run driven by 20 km global run turned out to be the best nesting approach in this study.



## 참고문헌

- 김옥연, 2004: 강수진단모델(Quantitative Precipitation Model)을 이용한 한반도의 단기 강수예측, 이학석사 학위논문, 부경대학교 대학원.
- 정유림, 2010: SRES A1B 시나리오를 이용한 한반도 수계별 강수 변화 모의, 이학석사 학위논문, 부경대학교 대학원.
- Bell, R. S., 1978: The forecasting of orographically enhanced rainfall accumulations using 10-level model data. *Meteor. Mag.*, **107**, 113-124.
- Bhowmik, S. K. R., D. Joardar, and H. R. Hatwar, 2007: Evaluation of precipitation prediction skill of IMD operational NWP system over Indian monsoon region, *Meteorol. Atmos. Phys.*, **95**, 205-221.
- Collier, C. G., 1975: A representation of the effects of topography on surface rainfall within moving baroclinic disturbances. *Q. J. R. Meteor. Soc.*, 101(429), 407-422.
- Etherton, B. and P. Santos, 2008: Sensitivity of WRF forecasts for south Florida to initial conditions, *Weather and forecasting*, **23**, 725-740.
- Ferretti, R., T. Paolucci, G. Giuliani, T. Cherubini, L. Bernardini, and G. Visconti, 2002: Verification of high-resolution real-time forecasts over the Alpine region during the MAP SOP, *Q. J. R. Meteorol. Soc.*, **129**, 587-607.
- Gao, X., Y. Xu, Z. Zhao, J. S. Pal, and F. Giorgi, 2006: On the role of resolution and topography in the simulation of east Asia



- precipitation, *Theor. Appl. climatol.*, **86**, 173–185.
- Jankov, I. and W. A. G. JR., 2005: The impact of different WRF model physical parameterizations and their interactions on warm season MCS rainfall, *Weather and forecasting*, **20**, 1048–1060.
- Kim, J. Y., J. H. Oh, d. Y. Kim, and P. Sen, 2008: Prediction of rainfall with high-resolution QPF model using public-resource distributed computing. *Asia-Pacific J. Atmos. Sci.*, **44**, 287–296.
- Kim, O. Y. and J. H. oh, 2010: Verification of the performance of the high resolution QPF model for heavy rainfall event over the Korea peninsula, *Asia-Pacific J. Atmos. Sci.*, **46(2)**, 119–133.
- Mass, C. F., D. Ovens, K. Westrick and B. A. Colle, 2002: Does increasing horizontal resolution produce more skillful forecasts, *BAMS*, 407–430.
- Misumi, R., B. A. Bell, and R. J. Moore 2001: River low forecasting using a rainfall disaggregation model incorporating small-scale topographic effects, *Meteor. Appl.*, **8**, 297–305.
- Lee, S. W., D. K. Lee, and D. E. Chang, 2011: Impact of Horizontal resolution and cumulus parameterization scheme on the simulation of heavy rainfall events over the korean peninsula, *Adv. Atmos. Sci.*, 28(1), 1–15.
- Liu, H., D. L. Zhang, and B. Wang, 2010: Impact of horizontal resolution on the regional climate simulations of the summer 1998 extreme rainfall along the Yantze River Basin, *J. Geophy. Res.* **115**, 1–14.
- Park, J. G. and D. K. Lee, 2011: Evaluation of heavy rainfall model

- forecasts over the Korean peninsula using different physical parameterization schemes and horizontal resolution, *Adv. Atmos. Sci.*, **28(6)**, 1233–1245.
- Shin, H. and S. Y. Hong, 2009: Quantitative precipitation forecast experiments of heavy rainfall over Jeju island on 14–16 September 2007 using the WRF model, *Asia-Pacific J. Atmos. Sci.*, **45(1)**, 71–89.
- Sinclair, M. R. 1994p: A diagnostic model for estimating orographic precipitation. *J. Appl. Meteorol.*, **33**, 1163–1175.
- WWRP/WGNE, 2012: Forecast Verification. This document is available at <http://www.cawcr.gov.au/projects/verification>, accessed 23 May, 2012.

